Green upconversion improvement of TiO2 codoped Er3+-Yb3+ nanoparticles based thin film by adding ALD-Al2O3 for silicon solar cell applications

Fatma Trabelsi, Frédéric Mercier, Elisabeth Blanquet, Alexandre Crisci, Raphael Boichot, Danying Chen, Rached Salhi

Green upconversion improvement of TiO_2 codoped Er^{3+}-Yb^{3+} nanoparticles based thin film by adding ALD-Al_2O_3 for silicon solar cell applications

Authors

Fatma Trabelsi [1,2], Frédéric Mercier [2], Elisabeth Blanquet [2], Alexandre Crisci [2], Raphael Boichot [2], Danying Chen [2], Rached Salhi [1]

Affiliations

1 Laboratory of Advanced Materials, National School of Engineers of Sfax, University of Sfax, 3038 Sfax, Tunisia

2 Univ. Grenoble Alpes, CNRS, Grenoble INP, SIMaP, 38000 Grenoble, France

*** Corresponding authors e-mail address:** fatma.trabelsi@grenoble-inp.fr

* **Telephone number**: +33 774969156

Abstract

This paper investigates the upconversion luminescence modification of codoped nanoparticles with lanthanides ions based thin films through adding a coating. First, these nanoparticles based thin films composed of Er^{3+}-Yb^{3+} co-doped anatase-TiO_2 are prepared using spin coating technique supported by a design of experiment (DOE) approach with the Hadamard matrix of order 4 to improve the deposition conditions. For the coating step, different thicknesses of Al_2O_3 layer are realised by thermal atomic layer deposition (T-ALD) onto the surface of Er^{3+}-Yb^{3+} co-doped anatase-TiO_2 nanoparticles based thin films. The results show that the ALD-Al_2O_3 coating can benefit the luminescence properties of the upconversion nanoparticles based thin films. Thin ALD-Al_2O_3 (10 nm) coated stack exhibits similar upconversion luminescence as the uncoated nanoparticles based film but insures also their stability. Meanwhile, for 100 nm ALD-Al_2O_3 coating, enhancement of the upconversion green emission by 98 % at the expense of the red emission compared to uncoated sample is observed. This results are promising to be applied in photovoltaics field.

Keywords

Upconversion; ALD; DOE; spin coating; TiO_2:Er-Yb; Al_2O_3

I. Introduction

In photovoltaic field, silicon solar cells have been the dominant driving force for the past several decades due to the relative abundance and environmentally friendly nature as no toxic heavy metals such as Cd or Pb are involved in their fabrication [1]. Nevertheless, one of the main drawbacks of silicon solar cells is the limited efficiency absorption of long wavelength sunlight. Moreover, silicon solar cells suffer from losses in power conversion efficiency due to non-radiative recombination of photo-generated charge carriers [2]. To address this issue, many efforts have been carried to improve cells absorption especially in infrared region. In this context, photon upconversion approach to improve solar energy conversion efficiency through expanding the absorption light range is adopted [3][4]. Upconversion luminescence is a nonlinear optical phenomenon that can convert low energy incident photons (near-infrared) to high energy (Visible) via absorbing two or more photons [5]. This high-energy photon is returned to the host solar cell where it can be reabsorbed [6]. The current upconversion study is focused on developing lanthanides doped nanopowder assembled as a layer suitable for enhancing the absorption efficiency of solar cells with low production cost. For the lanthanides ions, Er^{3+} shows green and red upconversion luminescence, but its weak absorption at the near-infrared wavelength gives low luminescence efficiency, which limits its applications. This problem is improved by adding Yb^{3+} ion that acts as a sensitizer. Yb^{3+} exhibits high absorption at 850 – 1050 nm, which enhances emission of Er^{3+} by transferring its energy to Er^{3+}. In addition, the efficiency of this phenomenon is associated with the host matrix due to the important role it plays in the energy transfer process. Moreover, TiO_2 co-doped Er^{3+}-Yb^{3+} is a transparent material with a high refractive index (n = 2.4) in visible wavelength, which is widely investigated for application in solar cells and photocatalytic fields [5], [7], [8]. In this research, TiO_2 is used as a host material.

The second step is to deposit upconversion nanoparticles on silicon substrate. Many techniques are frequently used to prepare films on flat materials (Langmuir– Blodgett, dip coating and spin coating). In this study, spin coating is used as a facile and low cost method with a full surface coverage [9]. Based on literature, the quality of spin coated films is influenced by three major factors: spinning speed, spinning time and volume. Therefore, in this study spin coating method is based on a design of experiment (DOE) approach, more precisely the screening method or Plackett–Burman two level design, to optimize process conditions and get the important information with the minimum number of experiments [10].

Although upconversion nanoparticles are an attractive wavelength converter, the luminescence is not very stable because of the high and sensitive surface area. Even exposure to ambient air can cause degradation of luminescence due to the surface impurities that create non-radiative trap states and lead to photoluminescence quenching that influences the device performance [11],[12]. To improve and stabilize luminescence efficiency, surface encapsulation is an effective way.

Surface passivation using dielectric Al_2O_3 layer deposited by Atomic Layer Deposition (ALD) process is known to provide outstanding effect of passivation on the surfaces of semiconductor. Al_2O_3 which is a negative charge dielectric film (introducing electric field) is used to reduce the non-radiative interface defect states and the electron or hole concentration [13],[14]. The benefits of atomic layer deposition are: the facile and precise thickness control, high uniformity over a wide area, and low deposition temperatures [15]. It is reported that effective passivation by ALD-Al_2O_3 requires an activating annealing under forming gas annealing (Ar/N_2 or N_2/H_2). Such H atoms will diffuse till the surface to further neutralize the interface defects leading to a reduction of the surface recombination rate of the generated photo-charge [16],[17]]. Therefore, the same structure and process provided for the enhancement of electrical properties for silicon solar cells will be kept with an integration of upconversion film between Si and ALD- Al_2O_3 layer followed by annealing under same conditions.

Nevertheless, ALD-Al_2O_3 deposition followed by heat treatment can also improve photoluminescence properties. Weifang et al. reported the photoluminescence intensity enhancement (up to 689%) through surface defects reducing of porous silicon carbide (B-N codoped SiC) by the passivation with 20 nm of ALD-Al_2O_3 followed with forming gas annealing (FGA) [18]. Chih-Yi et al. reported the stable luminescence under different power densities (23 and 128 kW/cm^2) and as a function of laser irradiation time in air and in vacuum of CdSe/ZnS quantum dots passivated with 10 nm of ALD-Al_2O_3 without post annealing treatment [19].

Here, we propose and demonstrate the viability of an efficient strategy to improve the green upconversion luminescence of lanthanide nanoparticles using ALD-Al_2O_3 layer followed by forming gas annealing treatment, by the intervention of point defects located in the band gap of Al_2O_3. The structure consists of an efficient upconversion Er^{3+}- Yb^{3+} co-doped TiO_2 nanoparticles deposited on Si substrate and then encapsulated with Al_2O_3 thin layer. First, as reported in a previous report : Er^{3+}- Yb^{3+} co-doped TiO_2 nanoparticles with anatase structure and 3-12 µm size with high surface area (140.6 m^2/g) are prepared using sol-gel method. Then

dispersion in a solvent and size reduction to ~ 9 nm with slight agglomeration (1 to 4 µm) is conducted based on electrostatic stabilization and physical dispersion (pH=3, ultrasonication for 30 min) [20]. This present work includes the next steps of the structure building procedure. First, the deposition of dispersed nanoparticles on n-type (100) silicon substrate using a spin coating technique is performed supported on design of experiments (DOE) approach. Then, improvement of spin coating cycles is conducted. Finally, Al_2O_3 layer is deposited by thermal ALD on the upconversion nanoparticles followed by annealing in forming gas at 430°C for 30 min as the suitable conditions for a good passivation performance of ALD-Al_2O_3 passivation layer based on the study of Wang et al. [21].

The structure, morphology and photoluminescence properties of spin coated nanoparticles and coated with various thickness of ALD-Al_2O_3 layer are systematically investigated. The evolution of the upconversion luminescence after every step is discussed in details.

II. Experiments details

1. Spin coating of upconversion nanoparticles

A soft chemistry route based on hydrothermal-assisted sol-gel method is used for the synthesis of 5 at.%Er - 5 at.%Yb co-doped anatase-TiO_2 nanoparticles that will be labelled TiO_2:Er-Yb. Then, dispersion in absolute ethanol under different operating conditions is carried out. These two steps are detailed in a previous report [20]. The substrates are n-type (100) Si wafers (CZ, thickness 250-300 µm and a resistivity 10-30 Ω.cm from Sil'tronix ST) cut in 20 mm × 20 mm pieces. Prior to spin coating deposition, the substrates are cleaned with conventional Radio Corporation of America procedure (RCA) [22]. The deposition process while respecting DOE approach is performed. More details on the experimental steps of the DOE approach used can be found in a previous study [23]. After deposition, the substrates are pre-heated on a heating plate for 1 min at 200°C in order to evaporate the rest of the solvent. The spin coated TiO_2:Er-Yb on Si substrate will be labelled as Si/TiO_2:Er-Yb. So, every spin coating cycle consists of deposition and pre-heat treatment. The deposition is conducted immediately after the substrate cleaning. The solution is dropped into the center of the substrate using a micropipette (100 µL -1000 µL) (Fig.1).

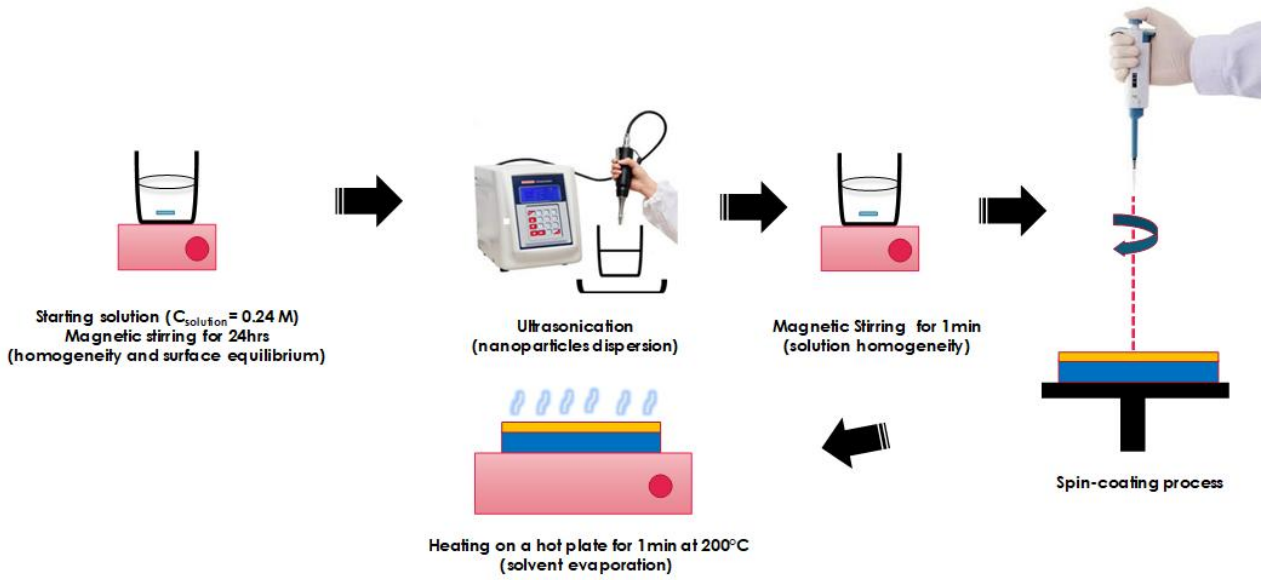

Fig. 1: Spin coating steps used.

Surface quality of the films is successfully evaluated using DOE approach. This method is used to extract the influence of the spin-coating process parameters around a central point (see supplementary data Table S.1, Fig. S1 and Fig. S2). All experiments and characterization are performed in a limited period (3 weeks). The GNU Octave 5.1.0 program was used to process the DOE dataset. For the desired response, the target is the minimum number of huge particles defined as particles with a size greater than 400 nm on the surface of Si.

The number of huge particles is measured in 3 different areas: center (C: 10 mm), intermediate (I: 5 mm) and border (B: 2 mm) (Fig. S1). In every area three images are taken randomly to check the homogeneity in every point. All images are taken in black and white to separate background from the particles of interest to facilitate their treatment with the public domain program ImageJ [24,25].

2. ALD-Al_2O_3 coating on upconversion nanoparticles based thin film

Coating with ALD is examined in order to study the influence of Al_2O_3 thickness followed by post heat treatment on structure and luminescence properties of TiO_2:Er-Yb. ALD-Al_2O_3 deposited on upconversion nanoparticles based thin films is performed in a home-made ALD reactor. Trimethylaluminium (TMA) and ultra-pure water are used as the precursor and oxidant, respectively. The reactor temperature is set to 200 °C during deposition, which is within the preferred ALD growth window of Al_2O_3. Nitrogen is used as the purge and the carrier gas with a flow rate of 100 sccm. Each cycle consists of a 1.5 s of TMA injection with a 30 s purge time, followed by a 1 s pulse of H_2O injection with a 60 s purge time. 62 and 620

cycles has been selected as the cycle numbers for ALD-Al_2O_3 deposition leading to 10 nm and 100 nm of thickness.

The post deposition annealing is an essential step to enhance the performance of various optoelectronic and photovoltaic devices. Therefore, an annealing treatment of the nanoparticles based thin films coated with ALD-Al_2O_3 is performed in a reducing gas atmosphere using forming gas (FGA) (N_2:H_2 / 95:5) at 430°C for 30 min. The ALD-Al_2O_3 coated on Si/TiO_2:Er-Yb followed by FGA will be labelled as Si/TiO_2:Er-Yb/62+FGA and Si/TiO_2:Er-Yb/620+FGA for 62 cycles and 620 cycles respectively.

3. Characterization

X-ray diffraction (XRD) patterns for all samples are performed on a BRUKER D8 Advanced diffractometer (SeriesII-2009) with Cu Kα radiation (λ=1.5418 Å). Cross-section TEM samples are prepared using Focused Ion Beam (FIB) technique. ACOM–TEM (Automated Crystal Orientation Mapping in Transmission Electron Microscopy) [26] is performed for phase and orientation mapping down to the nanometer scale (probe size of 1.6 nm). The data acquisition is carried out in a JEOL-2100F transmission electron microscope operated at 200 kV.

Photoluminescence spectra of the powder phase and uncoated Si/TiO_2:Er-Yb films under different number of spin coating cycles are recorded with a Jobin-Yvon T64000 spectrometer under excitation of laser at a wavelength of 514 nm with a power of 20 mW.

The room temperature upconversion spectra at a wavelength (λ) of 980 nm are assessed in a Jobin Yvon Fluoromax-4 Spectrofluorometer (Horiba, USA) with a 150 W Xe lamp as a source of excitation.

Histogram derived from PL spectra is based on the comparison of areas. The area of every peak is extracted from PL spectra using OriginPro 2017, section “integrate peaks”.

III. Results and discussion

1. Uncoated nanoparticles based thin films

1.1 DOE approach

From Fig. S.3 (supplementary data), a positive value in the model for a response represents an effect that favours and negative value indicates an inverse relationship between response and a factor. Table 1 gives the impact of each factor on the value (not on the desirability) of the

response. First, it is shown that the three studied factors have an influence on the deposit quality. Second, to achieve the minimum number of huge particles (> 400 nm) on Si surface, the response must have a negative value since we aim to decrease not to increase the number of huge particles. In addition, the parameter weight for the three factors is negative (see Fig. S.3). So, the three parameters must be at +1 level to get the desired response (see *Equation 1*.supplementary data). This result revealed that the spinning speed, time and volume of the colloidal suspension must be simultaneously increased to obtain a minimum number of huge particles with minimum size of 400 nm on the surface of Si substrate.

Table 1. Level of impact of factors on responses.

Factor	**Spinning speed**	**Spinning time**	**Volume**
Center	no effect	+	+
Intermediate	+	no effect	+
Border	no effect	no effect	+

±: negative or positive influence (above 2σ)

1.2 Spin coating cycles influence on PL response

An important target for investigation is to maintain the upconversion luminescence response of nanoparticles after the spin-coating deposition. The crucial factor that controls this emission is the spinning cycles amount [27]. For that purpose, the number of spin coating cycles is varied between 2 and 8. Between 2 cycles, the sample containing nanoparticles is heated at 200°C for 1 min. As it can be seen from the SEM micrographs presented in Fig.2, the total surface of the substrate is well covered with nanoparticles as the cycle number increases up to 8. As estimated from cross sectional SEM measurements, more coating cycles can result in a larger film thickness which are found to be between 265 ± 21 nm, 326 ± 44 nm and 713 ± 89 nm for 2, 4 and 8 cycles respectively. The measured thicknesses are the average values of three thicknesses in three different areas. It is worth mentioning that from this work and the literature data, the thickness deposited with spin coating process cannot be perfectly controlled through varying cycle numbers**.** In addition, it is interesting to note that during the preparation of the cross-section samples, the nanoparticles based films detached from the substrate (yellow arrow in Fig. 2). Based on the comparison between measured thicknesses in this study and other reports, it can be concluded that the thicknesses are in the same order with other reports. In fact, increasing cycle numbers gives a compact film with a total surface coverage. It also provides a relatively larger amount of fluorescent sites that is beneficial and

leads to the increase of PL intensities (Fig 3a and Fig 3b) [27]. Therefore, adjusting the number of spin-coated layers to 8 is optimum for preparing an upconversion nanoparticles based thin film while getting an optical response as the powder phase with full coverage of the substrate and compact film. This result is in good agreement with the literature: Srinatha et al reported the deposition of Al-doped ZnO nanoparticles on glass substrate (2.54×2.54 cm^2) using sol-gel spin coating (3000 rpm- 60 s-10 cycles) with thicknesses between 400 and 500 nm. The higher intensity of PL emission is shown with the thicker film [28]. Another paper mentioned that spin coating of TiO_2 film (3000 rpm-15 s) on TCO substrate (2.5×2.5 cm^2), with a thickness of about 0.92 µm (8 cycles) and 1.07 µm (10 cycles), have a higher PL emission than 4 and 6 cycles [29]. In addition, it is found that increasing thickness above 2.9 µm decreases the performance of nanoparticles (Cu_2SnSe_3) which are deposited by drop casting into FTO substrate due to more defects in thicker films [30].

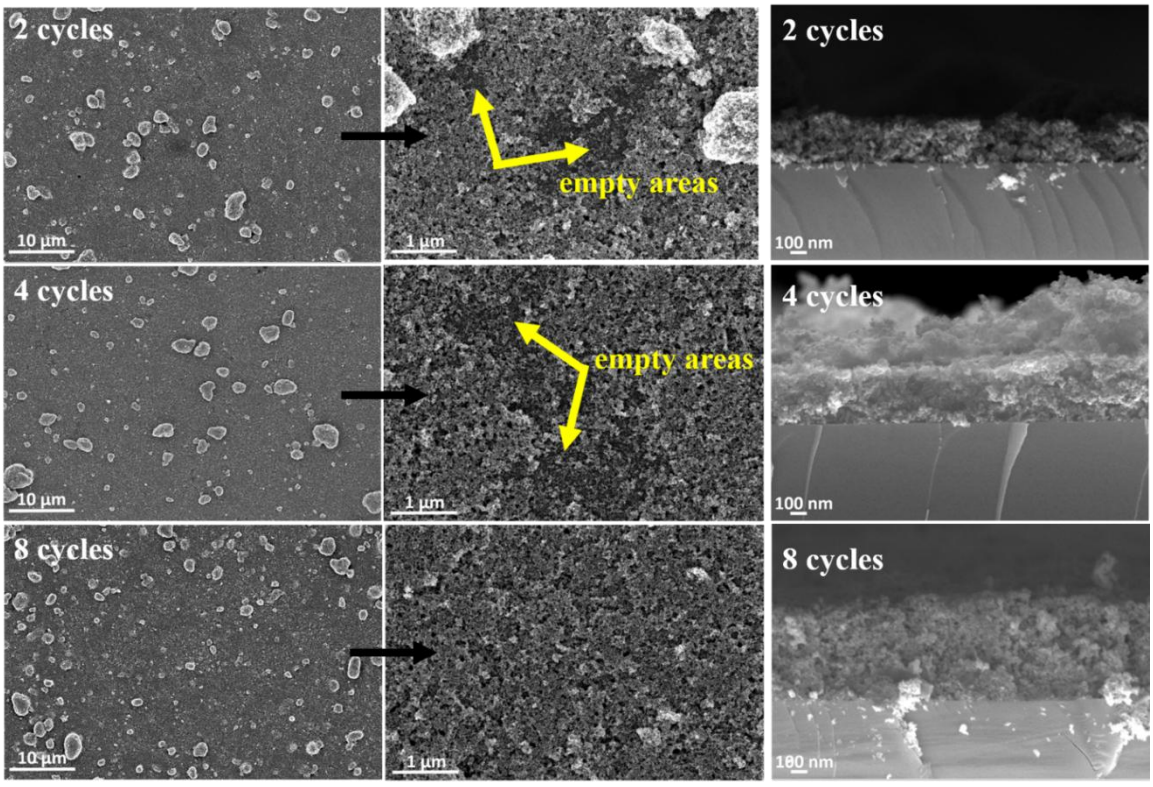

Fig. 2: SEM Top view images and cross sections of Si/TiO_2:Er-Yb with different spin-coating cycle numbers (2, 4 and 8).

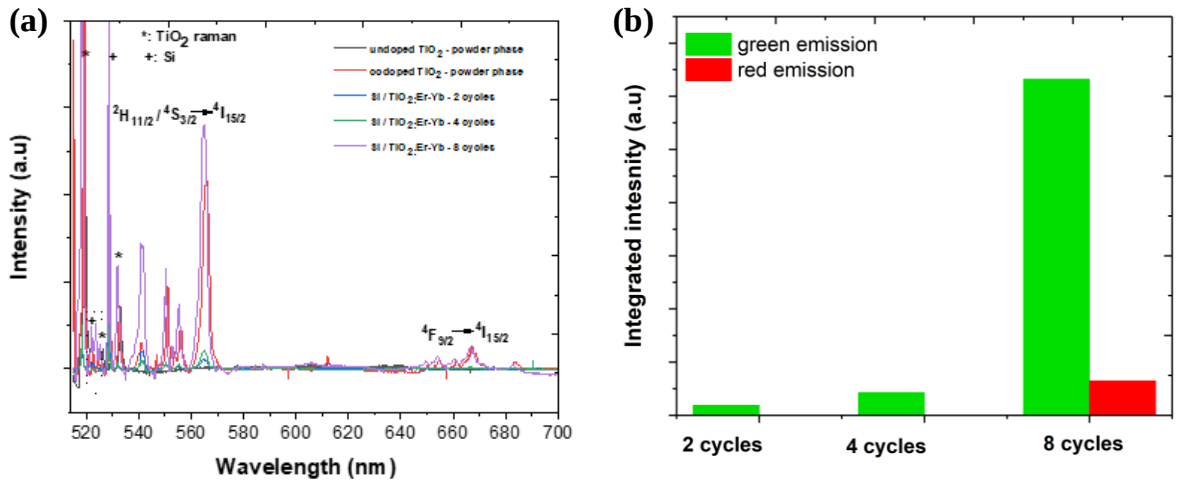

Fig. 3: (a) PL emission under excitation wavelength λ=514 nm of all the different samples from nanoparticles in powder phase to based thin film and (b) the corresponding integrated intensity of the peaks.

2. ALD-Al_2O_3 coated on nanoparticles based thin films

2.1 Morphology

The resulting films are cleaved and examined by SEM. According to the cross sectional SEM images (Fig. 4), the films are composed of a dense arrangement of nanoparticles, the thickness of the films ranging between 650 and 950 nm with a porous microstructure. Fig. 5 depicts the HR-TEM images, it can be seen that different measured thicknesses ranging from 19-21 nm and 100-130 nm are found for the Si/TiO_2:Er-Yb/62+FGA and Si/TiO_2:Er-Yb/620+FGA, respectively. It is difficult to determine exactly the film thickness. This thickness scattering can be explained by the roughness of the nanopowder that composes the porous film. In addition, it seems that TiO_2:Er-Yb nanoparticles are embedded in Al_2O_3 film, which can explain the difficulty of thickness measurements.

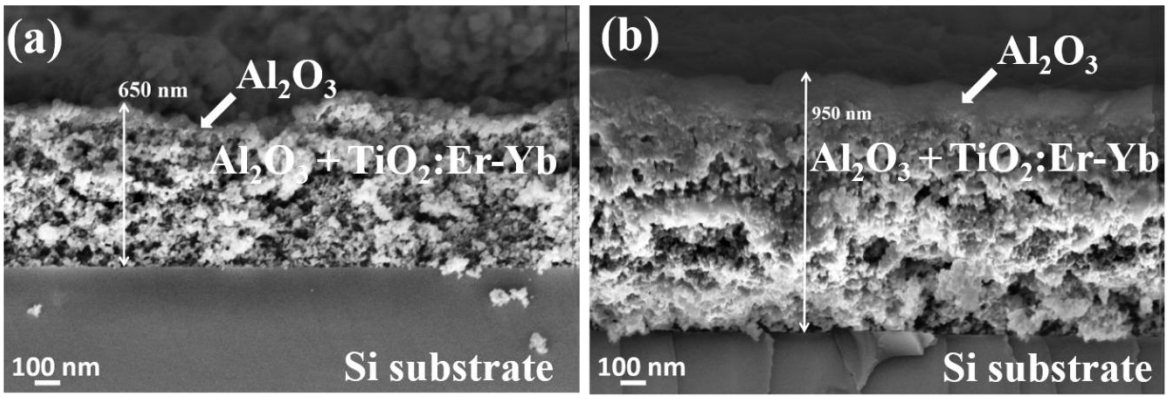

Fig. 4: SEM top view images of (a) Si/TiO_2:Er-Yb/62+FGA and (b) Si/TiO_2:Er-Yb/620 +FGA films.

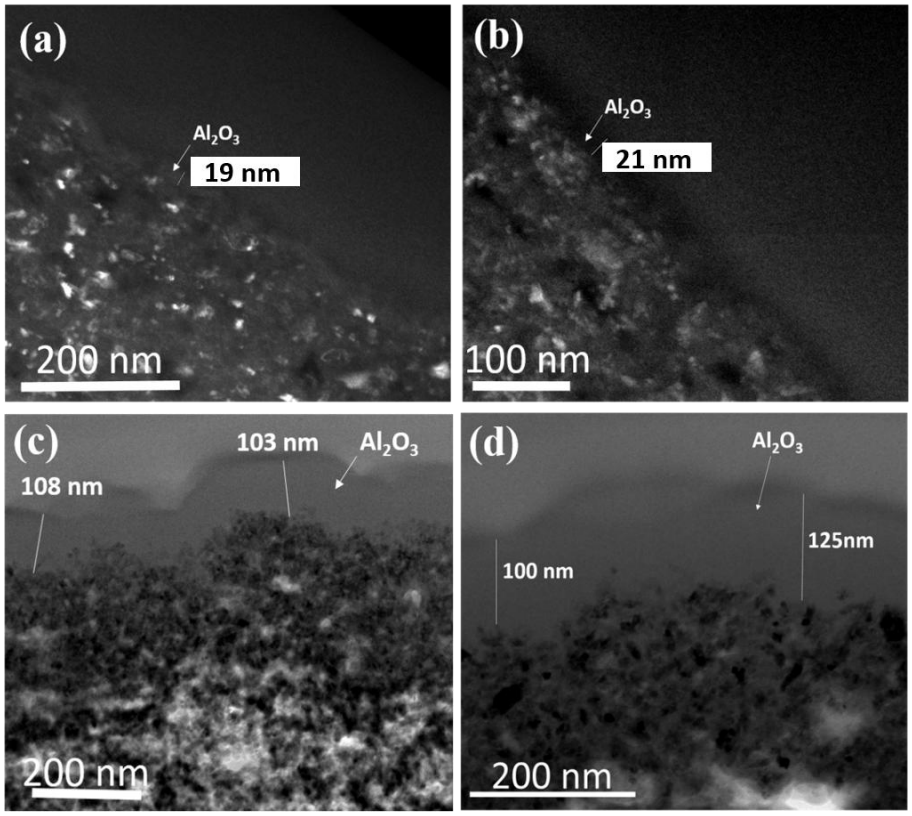

Fig. 5: HR-TEM images showing the thickness of (a, b) Si/TiO_2:Er-Yb/62+FGA, (c, d)) Si/TiO_2:Er-Yb/620+FGA films.

2.2 Structure

The influence of the ALD-Al_2O_3 coating on crystal structure of the different films is evaluated. The XRD patterns of Si/TiO_2:Er-Yb coated with different thicknesses of ALD-Al_2O_3 layer followed by FGA treatment are given in Fig. 6. Each pattern peaks are indexed for the anatase phase by comparison with the ICDD card number: 21-1272, indicating that all samples are constituted by a single crystalline anatase phase. No other phases such as rutile,

Er_2O_3, Yb_2O_3 is evidenced. For the ALD-Al_2O_3 layer, it is demonstrated in literature that deposition in the temperature range of 200°C-500°C and film thickness up to 200 nm, leads to the formation of an amorphous structure of Al_2O_3 [33]. This amorphous structure can be confirmed by the dark and bright field TEM images.

Crystallite size of the deposited nanopowders on Si substrate and coated with different thickness of ALD –Al_2O_3 followed by FGA treatment is calculated using Scherrer method, for the (101) and (200) diffraction detected planes. The results of microstructural parameters of the samples are presented in Table 2. The mean crystallite size remains almost the same until the end of the procedure. The ALD –Al_2O_3 layer acts as a buffer layer to suppress the growth of particles, which results in the same crystallite size [34].

These results confirm that until the end of the procedure no remarkable increase in the crystallite size is observed. The procedure proposed in the present study is efficient compared to the work conducted by Yogita et al. [35] that shows an increase of the crystallite size of pure TiO_2 nanoparticles synthesized by sol-gel method by 111% upon an annealing at 500°C-1h.

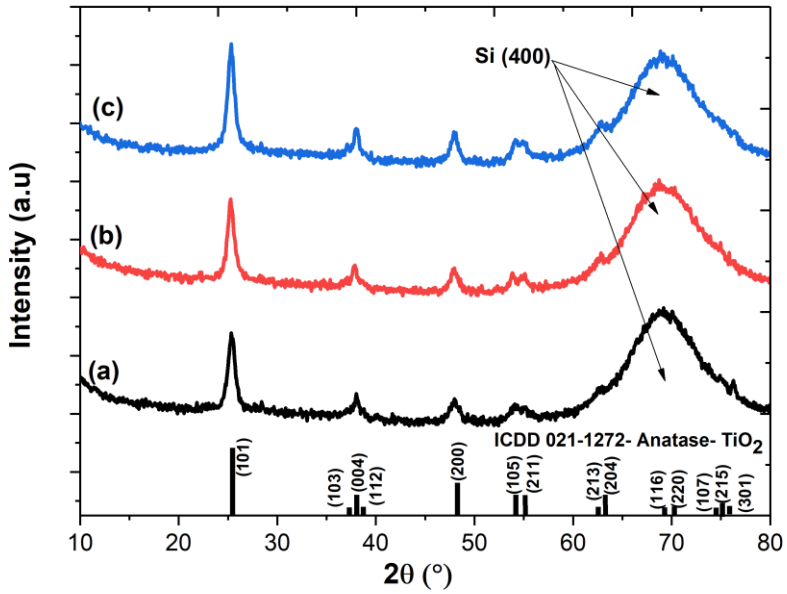

Fig. 6 : XRD patterns of: (a) Si/ TiO_2:Er-Yb, (b) Si/ TiO_2:Er-Yb / 62+ FGA and (c) Si/ TiO_2:Er-Yb/620+ FGA films.

Table 2. Microstructural parameters of the nanoparticles based thin films uncoated and coated with different thickness of ALD-Al_2O_3 layer from XRD patterns.

Sample	Mean crystallite size by Scherrer formula (nm)	a (Å)	c (Å)	c/a ratio	Unit cell volume (Å^3)
Si/TiO_2:Er-Yb	11	3.7911	9.4638	2.4963	136.02
Si/TiO_2:Er-Yb/62+FGA	11	3.7901	9.5076	2.5085	136.58
Si/TiO_2:Er-Yb/620+FGA	12	3.7911	9.4638	2.4963	136.02

To get an insight into the phase purity, the ACOM measurements are performed on Si/TiO_2:Er-Yb/620 film before and after FGA. Phase maps by combining anatase and a generic of rutile, aluminium titanate (Al_2TiO_5), pyrochlore (Er/$Yb_2Ti_2O_7$) erbium and ytterbium oxides (Er_2O_3 and Yb_2O_3) phases are constructed. No rutile nor pyrochlore phases are detected. From the results presented from Fig. 7, it is clearly seen from the phase map combined with index that every grain is indexed. It reveals the coexistence of aluminium titanate and erbium and/ ytterbium oxides. These phases are still present even when combining reliability with index and phase maps. Obviously, these phases have appeared during the ALD process at low temperature (200°C) with process duration of 17 hours. The reliability factor, which measures the ratio between the correlation indexes related to the two solutions has a poor value (<15). Therefore, we cannot differentiate between erbium and ytterbium oxides. These oxides have similar crystallographic response (same crystal system (cubic), space group (Ia-3)) and small crystallites size (~ 10 nm).

This observation for the Si/TiO_2:Er-Yb/620+FGA sample is not in agreement with the corresponding XRD pattern, which proves that these secondary phases have small concentrations and sizes below the level of detection of the XRD instrument [36]. The formation of Al_2TiO_5, crystallizing in the orthorhombic system with the space group Cmcm and the following lattice parameters a = 3.591Å, b = 9.429Å and c = 9.636Å, may be explained by the substitution of Er^{3+} or Yb^{3+} sites by Al^{3+} in the TiO_2 lattice. Due to its smaller ionic radius (0.535 Å), Al^{3+} can be inserted into anatase. Here, we present a possible diffusion into the volume. For the codoped TiO_2, as the dopants (Er^{3+} and Yb^{3+}) present a different charge than Ti^{4+}, oxygen vacancies can be created to compensate the missing charges. These defects can influence the diffusion rate by changing the concentrations of point defects. More vacancies make it easier for ions to move [37]. It is reported that Al is able to diffuse interstitially in TiO_2. Zhao et al [38] show the creation of Al_2TiO_5 from amorphous TiO_2 with Al^{3+} interstitials. Kokestsu and co-workers present DFT study on

reversible insertion of Al^{3+} and Mg^{2+} in Ti vacancies in anatase TiO_2 monovalent doped with F^- and OH^- for use as electrode material for practical multivalent batteries [39].

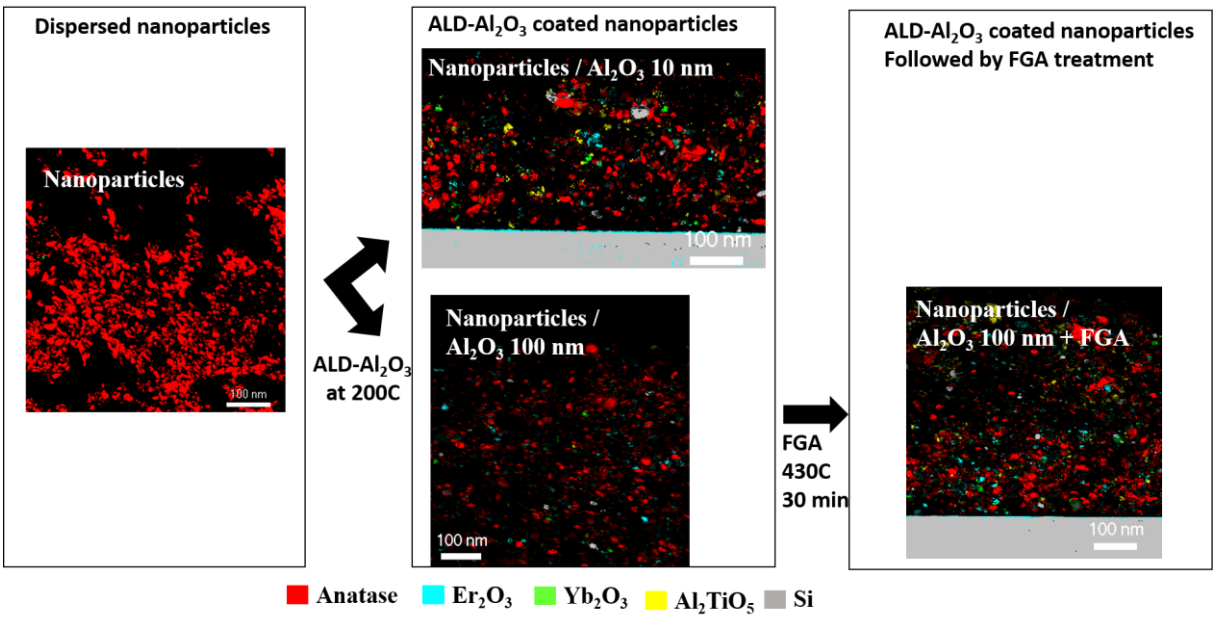

Fig. 7: ACOM-TEM phase maps of nanoparticles at different stages of the process

2.2 Upconversion luminescence

The upconversion luminescence properties of the uncoated and coated TiO_2:Er-Yb nanoparticles based thin films are studied in order to understand the influence of ALD-Al_2O_3 coating thickness and post heat treatment, which are necessary steps towards the improvement of the efficiency of Si based solar cells.

Fig.8 a**,** b display the upconversion luminescence spectra at room temperature under 980 nm excitation of the TiO_2:Er-Yb nanoparticles deposited on Si substrate and coated with different thicknesses of ALD-Al_2O_3 followed by FGA. The SEM images in Fig. 8 c, d show the stack buildings evolution from nanopowder form to coated thin film. It can be seen that the same upconversion emissions regions for the all the samples are observed proving that the basic optical behavior of the material has not been changed by the coating followed by FGA treatment. Two emission regions can be distinguished. The emissions centered at 544 nm (green region), 584 nm (green region), 620-686 nm (red region) are originated from $^2H_{11/2} \rightarrow {}^4I_{15/2}$, $^4S_{3/2} \rightarrow {}^4I_{15/2}$ and $^4F_{9/2} \rightarrow {}^4I_{15/2}$ transitions, respectively as have already been reported by many studies [40],41. The presence of f-f transitions of Er^{3+} and the strong absorption of Yb^{3+} ($^4F_{7/2} + h\upsilon_{980nm} \rightarrow {}^4F_{5/2}$) sustain the effective incorporation of the lanthanide dopants into TiO_2 lattice.

The proposed mechanism of upconversion emission have been widely discussed previously in the literature and it is originated from two-photon UC process: The $^2F_{5/2}$ (Yb^{3+}) and $^4I_{11/2}$ (Er^{3+}) levels are in energetic resonance. Since the absorption cross-section of the $^2F_{7/2} \rightarrow {}^2F_{5/2}$ transition of Yb^{3+} ion, corresponding to IR absorption at 980 nm, is much larger than that of the $^4I_{15/2} \rightarrow {}^4I_{11/2}$ transition of Er^{3+} ion, the ETU mechanism is the most dominant process. Therefore, upon 980 nm laser excitation, Yb^{3+} ions can efficiently transfer their energy to Er^{3+} populating the $^4I_{11/2}$ excited state of neighboring Er^{3+} and then relax to the ground state $^2F_{7/2}$. Then the Er^{3+} ion populated in $^4I_{11/2}$ captured the photon from second surrounding Yb^{3+} ion and jumped to $^4F_{7/2}$ higher energy level through ESA. However, due to the short life time of the $^4F_{7/2}$ level in Er^{3+}, non-radiative multiphonon process to the lower $^2H_{11/2}$ and $^4S_{3/2}$ levels takes place due to the small energy distance between them. Then a relaxation of the populated levels to the ground state $^4I_{15/2}$, resulting in the green emission.

The observed red emission is generated from non-radiative relaxation from the $^4S_{3/2}$ to $^4F_{9/2}$ level and cross relaxation process (CR): $(Er^{+3})\ ^4F_{7/2} + (Er^{+3})\ ^4I_{11/2} \rightarrow (Er^{+3})\ ^4F_{9/2}$. The intensity of the red emission is lower than that in green can be explained by the weak absorption cross relaxation [42] 43. No apparent modification on peak positions (similar emission bands) after the deposition of powder on Si substrate, coating and post heat treatment steps can be observed except increment in their intensities, which suggests that that the upconversion mechanism is not changed.

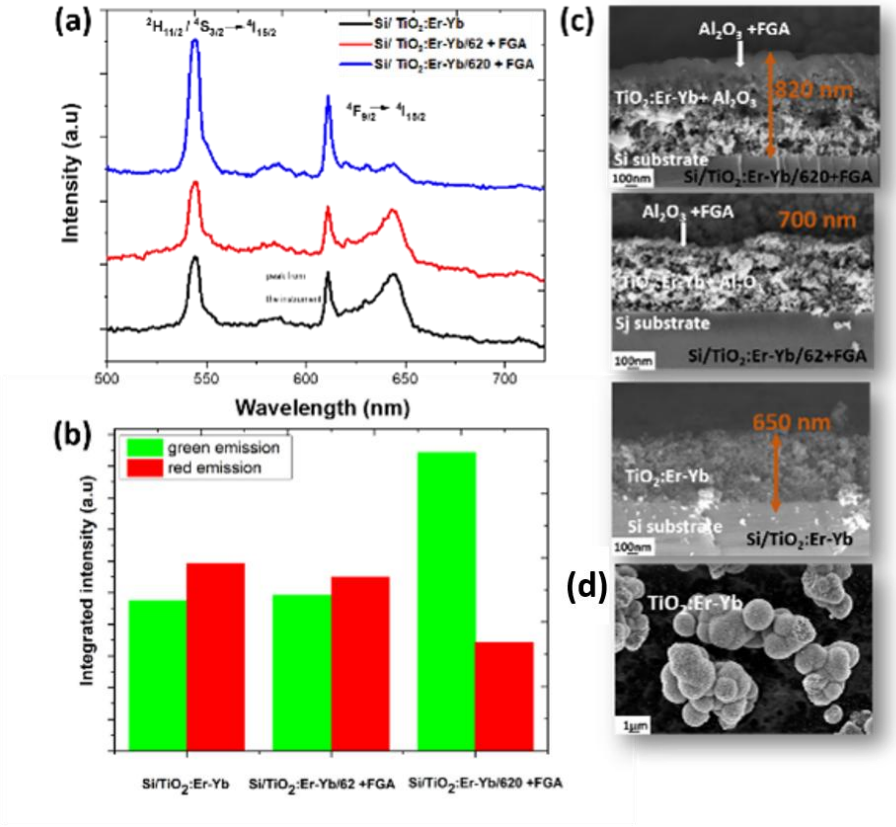

Fig. 8 : (a) Visible upconversion emission spectra of TiO_2:Er-Yb nanopowder deposited on Si substrate and coated with different thicknesses of Al_2O_3 +FGA using 980 nm laser excitation source,(b) Histograms of green and red emissions integrated intensities, (c) cross sectional SEM micrographs of different films and (d) SEM micrographs of sol-gel elaborated TiO_2:Er-Yb nanopowder.

As shown in Fig.8 b, maintaining of the initial emissions intensities with the thin ALD-Al_2O_3 layer (62 cycles + FGA) compared to uncoated film is ensured. Applying ALD-Al_2O_3 layer on nanopowder based thin films appears to have no effect on upconversion luminescence. It can be explained by the fact that the deposited layer acts as a barrier preventing the nanopowder

surface from the surrounding environment, which leads to the maintaining of the same emissions. By increasing the cycle numbers to 620 (thick layer), the incident illumination and the emitted light can be slightly obstructed by the protective coating, thus the intensity of upconversion emissions as for the red one decreased. Meanwhile, the green emission peak intensity is drastically enhanced by about 98% compared to uncoated nanoparticles based thin film. Same observation is reported elsewhere with the increasing of annealing temperature of the nanopowder, which is explained by the change in the crystalline field at the optical centers [44].

In the present study, this increasing of green emission could originate from the density of the defects in ALD-Al_2O_3 layers such as Er_2O_3-Yb_2O_3-Al_2TiO_5 may contribute to the increase of the green emission. The intrinsic point defects within the electronic band gap generated in Al_2O_3 layer during ALD process. As reported in [45–49], amorphous Al_2O_3 layer grown by ALD process contain: interstitial oxygen (O_i)/aluminium (Al_i), vacancies of oxygen (V_O)/aluminium (V_{Al}), and also interstitial hydrogen (H_i) defects, that occupied energy levels in the band gap amorphous-Al_2O_3. After annealing of the layer, it is assumed that interstitial oxygen (O_i) and aluminium vacancies (V_{Al}) are predominantly present, which cause the negative charging of amorphous Al_2O_3 film used for the passivation of Si solar cells. So, the underlying reason for UC enhancement may be caused from this defects that occupied levels near to the valence band. The density of these defects increase with thickness of the layer. These defects that will make from Al_2O_3, that is coated around the particles and diffused along the whole film (Fig. 9 a), an absorption center that ensure an additional energy transfer to Er^{3+} ions after being excited with 980 nm (Fig.9 b). Subsequently, UC nanopowder emitted an intense green emission after a combination of a direct (from Yb^{3+}) and indirect (from Al_2O_3) excitation.

It should be pointed that the formation of secondary phases as shown by ACOM-TEM, can not have a drastic influence on the improvement of upconversion luminescence first due to the low amount of these phases that could not be detected by XRD or quantified by ACOM-TEM. Second, concerning theses phases, Al_2TiO_5 absorb only in UV region (under 400 nm). For Yb_2O_3, it absorbs and emits at 980 nm, the emitted photons can probably be reabsorbed after that by codoped TiO_2 or even by Er_2O_3. For Er_2O_3, the Er^{3+} ion alone can achieve luminescence without the requirement of a sensitizer that means no ETU process is present (weak efficiency compared to when using a sensitizer) [50]. The energy of the 980 nm

matches the absorption energy level between $^4I_{15/2}$ ground state and $^4I_{11/2}$ excitation state of Er^{3+}.

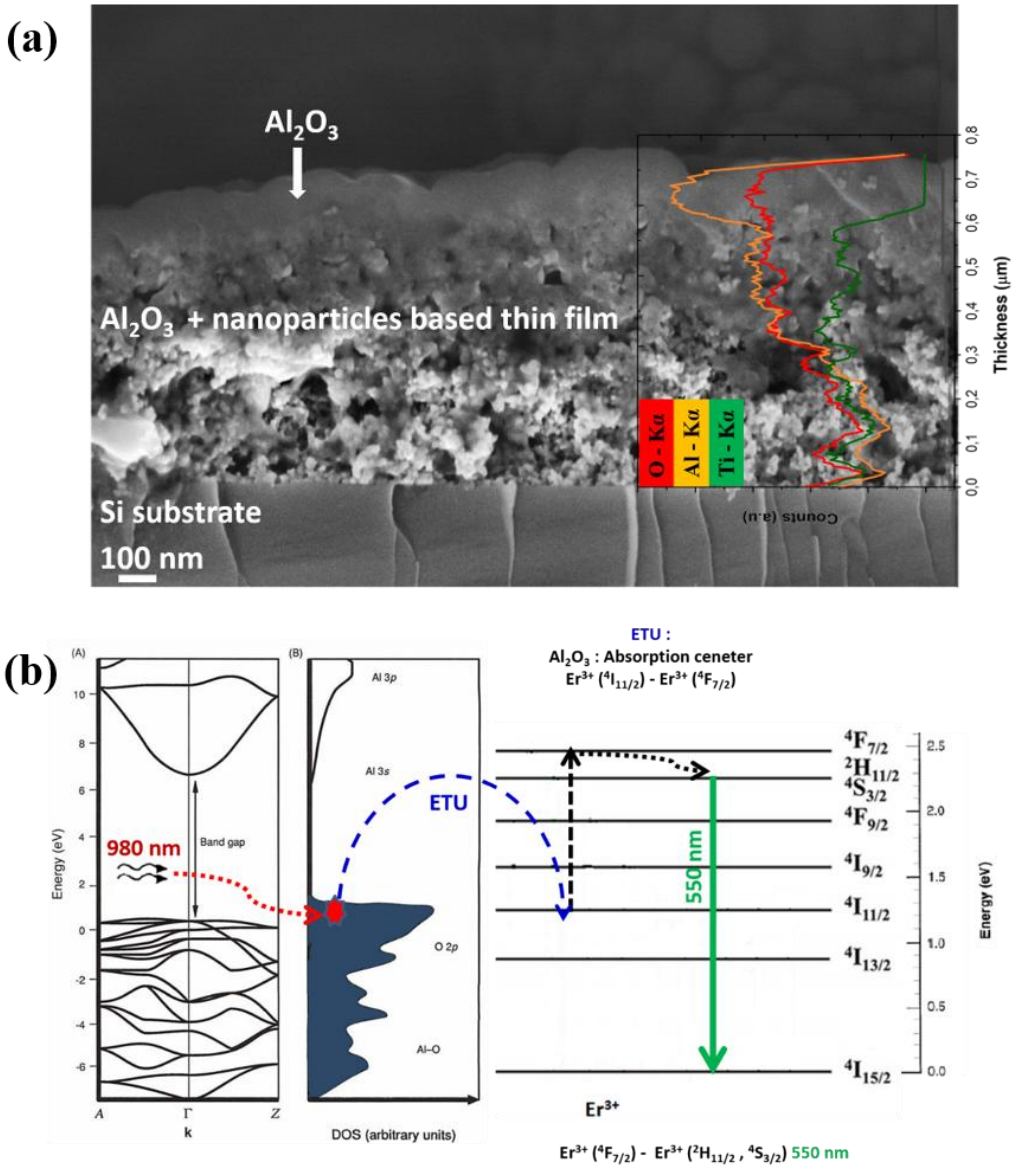

Fig. 9 : (a) SEM image of Si/TiO_2:Er-Yb/620 +FGA combined with line profile graph for Al and O elements presence along the film and (b) The probably mechanism for the indirect excitation of Er^{3+} ions by ALD-Al_2O_3 layer.

Reflectivity ratio (related to standard Si substrate) of the two different thicknesses ALD AL_2O_3 stack(Table. 3) demonstrate that using thicker layer of Al_2O_3 reduces the reflectance of the structure especially at 950 nm (decreasing of about 54%), which is the same wavelength as the excitation source, so increasing the absorption of photons which lead to an increase of upconversion emission. The low reflection value on the 400 to 1100 nm spectrum range is

highly desirable as it can lead to the absorption enhancement in thin film solar cells [50]. A structure with these properties would increase the solar cell efficiency combining upconversion and anti-reflectivity, which is similar to as recently reported in [8].

Table 3. Reflectivity measurements of the two-coated samples with different thickness of ALD-Al_2O_3 + FGA.

Samples	**Ratio of Reflectivity % Film/silicon substrate at 950 nm (photons not absorbed)**
Si/ TiO_2:Er-Yb / 62 + FGA	13.5
Si/ TiO_2:Er-Yb / 620 + FGA	6.2

Conclusions

In this work, upconversion nanoparticles based thin film composed of Er^{3+}-Yb^{3+} co-doped anatase-TiO_2 is successfully elaborated via spin coating route based on design of experiment (DOE) approach. The increase of spinning speed, time, volume and number of cycles lead to a film with minimum number of huge particles (>400 nm) on surface of substrate and luminescence response similar to the initial powder. Applying a thin layer of ALD–Al_2O_3 has no influence on luminescence phenomena by maintaining the upconversion luminescence as the uncoated nanopowder based thin film. The increase of ALD–Al_2O_3 thickness is found to strengthen the green upconversion luminescence intensity in comparison to that of thinner one due probably to the intrinsic defects intervention. This work confirms that selective upconversion luminescence can be assured by tuning the thickness of ALD-Al_2O_3 followed by FGA treatment. The reason behind this enhancement is identified, and will be further investigated. From our study, we believe that the application of this structure to the solar cells is a truly viable approach to achieve higher device efficiency at temperature below 450°C.

Acknowledgement

The authors would like to thank: Rachel Martin and Thierry Encinas from C.M.T.C for their support in SEM characterizations and XRD patterns analysis, respectively. Electron microscopy is performed at the CMTC characterization platform of Grenoble INP supported by the Centre of Excellence of Multifunctional Architectured Materials "CEMAM" n°AN-10-

LABX-44-01 funded by the "Investments for the Future" Program. The authors would like to thank Laure Cointeaux from Grenoble INP, LEPMI for her help for providing the dispersion equipment.

This work is part of the French network on ALD (GDR RAFALD- CNRS-CEA).

References

[1] A. Khare, A critical review on the efficiency improvement of upconversion assisted solar cells, Journal of Alloys and Compounds 821(2020), 153214.

[2] S. Bhattacharya and S. John, Beyond 30% Conversion Efficiency in Silicon Solar Cells: A Numerical Demonstration, Nature 9 (2019), 12482.

[3] Manli Zhanga et al., Selective enhancement of green upconversion luminescence from $NaYF_4$:Yb, Er microparticles through Ga^{3+} doping for sensitive temperature sensing, Journal of Luminescence 215 (2019) 116632.

[4] V. Kumar, O. M. Ntwaeaborwa, T. Soga, V. Dutta, and H. C. Swart, Rare Earth Doped Zinc Oxide Nanophosphor Powder: A Future Material for Solid State Lighting and Solar Cells, ACS Photonics, 4 (2017) 2613–2637.

[5] Z. Yang, K. Zhu, Z. Song, D. Zhou, Z. Yin, and J. Qiu, Preparation and upconversion emission properties of TiO_2:Yb, Er inverse opals, Solid State Communications 151 (2011) 364–367.

[6] D. G. Sellers, J. Zhang, E. Y. Chen, Y. Zhong, M. F. D. N, and J. M. O. Zide, Novel nanostructures for efficient photon upconversion and high efficiency photovoltaics, Solar Energy Materials and Solar Cells 155 (2016) 446–453.

[7] X. Wang et al., Enhanced Photovoltaic Performance of Perovskite Solar Cells Based on Er-Yb Co-doped TiO_2 Nanorod Arrays, Electrochimica Acta 245 (2017) 839–845.

[8] R. Y. S. Zampiva et al., Luminescent anti-reflection coatings based on Er^{3+} doped forsterite for commercial silicon solar cells applications, Solar Energy 170 (2018) 752–761.

[9] Z. Welchel, L. A. DeSilva, and T. M. W. J. Banadara, Properties of tris (8-hydroxyquinoline) aluminum thin films fabricated by spin coating from static and dynamic dispense methods," Optical Materials 108 (2020) 110447.

[10] S. H. Lee et al., Synthesis of carbon nanotube fibers using the direct spinning process based on Design of Experiment (DOE)," Carbon 100 (2016) 647–655.

[11] G.De, W. Qin, J.Zhang, Y.Wang, C.Cao, Y.Cui, Effect of OH- on the upcomversion luminescent efficiency of Y_2O_3:Yb^{3+},Er^{3+} nanostructures, Solide state communications 137 (2006) 483-487.

[12] P.M. Ramos, Novel Erbium (III) and Ytterbium (III) based materials for optoelectronc and telecommunication applications (2013).

[13] H. Azizpour et al., Effective coating of Titania nanoparticles with alumina via atomic layer deposition, Applied Surface Science 426 (2017) 480–496.

[14] K. Cao, J. Cai, B. Shan, and R. Chen, Surface functionalization on nanoparticles via atomic layer deposition, Science Bulletin 65 (2020) 678–688.

[15] C. Barbos et al., Characterization of Al_2O_3 Thin Films Prepared by Thermal ALD, Energy Procedia 77 (2015) 558–564.

[16] I. Desnstorfer, T. Chohan, P.M Jordan, M. Knaut, D.K.Simon, J.W. Bartha and T. Mikolajick, Al_2O_3-TiO_2 nanolaminates for conductive silicon surface passivation, Journal of Photovoltaics 6(2016) 1.

[17] J. Hu and H.S Wong, Effect of annealing ambient and temperature on the electrical characteristics of atomic layer deposition $Al_2O_3/In_{0.53}Ga_{0.47}As$ metal-oxide-semiconductor capacitors and MOSFETs, Applied physics 111(2012) 0441

[18] L.Weiflang, I.Yoshimi, O.Yiyu, J.Daiki, K.Satoshi, P.P.Michael, O.Haiyan, Effective optimization of surface passivation on porous silicon carbide using atomic layer deposited Al_2O_3, RSC advances 7 (2019) 8090-8097.

[19] C. Y. Cheng and M. H. Mao, Photo-stability and time-resolved photoluminescence study of colloidal CdSe/ZnS quantum dots passivated in Al_2O_3 using atomic layer deposition, Journal of Applied Physics 120 (2016).

[20] F. Trabelsi, F.Mercier, E. Blanquet, A. Crisci, and R.Salhi, Synthesis of upconversion TiO_2:Er-Yb nanoparticles and deposition of thin films by spin coating technique," Ceramics international 46 (2020) 28183–28192.

[21] W. C. Wang, M. C. Tsai, J. Yang, C. Hsu, and M. J. Chen, Efficiency enhancement of nanotextured black silicon solar cells using Al_2O_3/TiO_2 dual-layer passivation stack prepared by atomic layer deposition, ACS Applied Materials and Interfaces 7 (2015) 10228–10237.

[22] C. T. Lu, Y. S. Huang, and C. W. Liu, Passivation of Al_2O_3/TiO_2 on monocrystalline Si with relatively low reflectance,Journal of Physics D: Applied Physics 49 (2016) 245105.

[23] R. Boichot et al., Epitaxial growth of AlN on (0001) sapphire: Assessment of HVPE process by a design of experiments approach, Coatings 7 (2017).

[24] N. Stolze, C. Bader, C. Henning, J. Mastin, A. E. Holmes, and A. L. Sutlief, Automated image analysis with ImageJ of yeast colony forming units from cannabis flowers, Journal of Microbiological Methods 164 (2019) 105681.

[25] M. Đuriš, Z. Arsenijević, D. Jaćimovski, and T. Kaluđerović Radoičić, Optimal pixel resolution for sand particles size and shape analysis, Powder Technology 302 (2016) 177–186.

[26] Rauch, E.F et al, Automated nanocrystal orientation and phase mapping in the transmission electron microscope on the basis of precession electron diffraction, Zeitshrift fur cristallographie 225 (2010) 103-109.

[27] A. Rodriguez-Gómez, A. García-Valenzuela, E. Haro-Poniatowski, and J. C. Alonso-Huitrón, Effect of thickness on the photoluminescence of silicon quantum dots embedded in silicon nitride films, Journal of Applied Physics 113 (2013).

[28] N. Srinatha, P. Raghu, H. M. Mahesh, and B. Angadi, Spin-coated Al-doped ZnO thin films for optical applications: Structural, micro-structural, optical and luminescence studies,Journal of Alloys and Compounds 722 (2017) 888–895.

[29] P. Malliga, J. Pandiarajan, N. Prithivikumaran, and K. Neyvasagam, Influence of Film Thickness on Structural and Optical Properties of Sol – Gel Spin Coated TiO_2 Thin Film," IOSR Journal of Applied Physics 6 (2014) 22–28.

[30] C. B. Song, Y. L. Zhao, D. M. Sogn, L. Zhu, X. Q. Gu, and Y. H. Qiang, Dye-sensitized solar cells based on TiO_2 nanotube/nanoparticle composite as photoanode and Cu_2SnSe_3 as counter electrode, International Journal of Electrochemical Science 9 (2014) 3158–3165.

[31] T. Keuter, N. H. Menzler, G. Mauer, F. Vondahlen, R. Vaßen, and H. P. Buchkremer, Modeling precursor diffusion and reaction of atomic layer deposition in porous structures, Joural of vacuum science and technology A 33 (2014).

[32] J. Guo, H. van Bui, D. Valdesueiro, S. Yuan, B. Liang, and J. R. van Ommen, Suppressing the photocatalytic activity of TiO_2 nanoparticles by extremely thin Al_2O_3 films grown by gas-phase deposition at ambient conditions, Nanomaterials 8 (2018).

[33] I. Iatsunskyi, M. K., M. Jancelewicz, K. Załęski, S. Jurga, and V. Smyntyna, Structural and XPS characterization of ALD Al_2O_3 coated porous silicon, Vaccum 113 (2015) 52–58.

[34] R. T. Sataloff, M. M. Johns, and K. M. Kost, Effective atomic interface engineering in $Bi_2Te_{2.7}Se_{0.3}$ thermoelectric material by atomic-layer-deposition approach. Nano Energy 49 (2018) 257-266.

[35] Y. Kumari, L. K. Jangir, A. Kumar, M. K. A, and K. Awasthi, Luminescent and structural behaviour of Tb^{+3} ions doped TiO_2 nanoparticles synthesized by facile sol-gel method, Physica B: Physics of Condensed Matter 602 (2021) 412465.

[36] Paweł Mazierskia et al., On the excitation mechanism of visible responsible Er-TiO_2 system proved by experimental and theoretical investigations for boosting photocatalytic activity, Applied Surface Science 527 (2020) 146815.

[37] J. Zheng, X. Hu, Z. Ren, X. Xue, and K. Chou, Solid-state reaction studies in Al_2O_3-TiO_2 system by diffusion couple method, ISIJ International 57 (2017) 1762–1766.

[38] Bingxin Zhao et al., The application of Al_2TiO_5 at the TiO_2/perovskite interface to decrease carrier losses in solar cells, Journal of materials chemisty A 28 (2017) 1487–1493.

[39] R. T. Sataloff, M. M. Johns, and K. M. Kost, Reversible magnesium and aluminum ions insertion in cation -deficient anatase TiO_2, Nature materials (2017).

[402] Y. Ledemi et al., White light and multicolor emission tuning in triply doped $Yb^{3+}/Tm^{3+}/Er^{3+}$ novel fluoro-phosphate transparent glass-ceramics, Journal of Materials Chemistry C 2 (2014) 5046–5056.

[41] S. Krause, M. Koerstz, R. Arppe-Tabbara, T. Soukka, and T. Vosch, NIR induced modulation of the red emission from erbium ions for selective lanthanide imaging, Methods and Applications in Fluorescence 6 (2018).

[42] R. Salhi and J. Deschanvres, Efficient green and red up-conversion emissions in Er/Yb co-doped TiO_2 nanopowders prepared by hydrothermal-assisted sol–gel process, Journal of Luminescence 176 (2016) 250–259.

[43] W. Bian, M. Zhou, G. Chen, X. Yu, M. Pokhrel, and Y. Mao, Upconversion luminescence of ytterbium and erbium co-doped gadolinium oxysulfate hollow nanoparticles, Applied Materials Today 13 (2018) 381–386.

[44] V. G. Ilves et al., Multimodal upconversion CaF_2 : Mn/Yb/Er/Si nanoparticles, Journal of fluorine chemistry 231 (2020) 109457.

[45] K. Henkel, M. Kot, and D. Schmeißer, Localized defect states and charge trapping in atomic layer deposited-Al_2O_3 films, Journal of Vacuum Science & Technology A 35 (2017) 01B125.

[46] T. V. Perevalov et al., Oxygen deficiency defects in amorphous Al_2O_3, Journal of Applied Physics 108 (2010) 013501.

[47] O. A. Dicks, J. Cottom, A. L. Shluger, and V. V. Afanas'Ev, The origin of negative charging in amorphous Al_2O_3 films: The role of native defects, Nanotechnology 30 (2019) 205201.

[48] Y. Gandhi, M. V. R. Rao, C. S. Rao, I. V. Kityk, and N. Veeraiah, Role of Al_2O_3 in upconversion and NIR emission in Tm^{3+} and Er^{3+} codoped calcium fluoro phosphorous silicate glass system, Journal of Luminescence 131 (2011) 1443–1452.

[49] S. Mingyi et al., "Effect of Yb^{3+} concentration on upconversion luminescence of AlON: Er^{3+} phosphors, Journal of rare earths 33 (2014) 227, 2014.

[50] R. Zhang et al., Fabrication and characterization of Al_2O_3/Si composite nanodome structures for high efficiency crystalline Si thin film solar cells, AIP Advances 5 (2015) 127209.